**Colloid & Polymer Science** Colloid Polym Sci 272:1043–1055 (1994)

# Comparative study of adsorption and heats of adsorption on planar and particulate polymer surfaces

L. Filippov

Selley G. Mudd Building, Lehigh University, 6 East Packer Avenue, Bethlehem, Pennsylvania 18015-3172, USA

*Abstract*: The adsorption and heats of adsorption of Lewis acidic-basic *probes* on planar and particulate surfaces of polyimide/siloxane, 6F photoimagable fluorinated polyimide and 6F polyimide have been studied by flow microcalorimetric, ellipsometric, and contact angle techniques. The heats of adsorption obtained by these techniques are in good agreement. It is noted that the ellipsometric method based on an analysis of adsorption kinetics has advantages over the contact angle technique and may be used for the study of the interface on planar polymer surfaces. The acidic-basic properties of polymers were approximately estimated by using the Drago *E* and *C* constants.

*Key words*: Adsorption – heats of adsorption – planar and particulate surfaces.

## Introduction

Most polymers have functional sites that are electron donors (base) or electron acceptors (acids). The acid-base interactions in adsorption onto the polymer surface involve both the acidic or basic sites of the adsorbate and the acidic or basic sites of the polymers. The heats of adsorption are entirely predictable as Lewis acid-base interactions between electron donors (such as sulfur, nitrogen, oxygen, etc.) and electron acceptors (such as iodine, phenol, etc.). Quantitative calorimetric studies of simple organic liquids by Drago and co-workers [1, 2] showed that enthalpy (or heat of adsorption) may be used to correlate and predict the enthalpy for several Lewis acid-base systems. This empirical correlation is presented by

$$-\Delta H^{ab} = \mathrm{E_A E_B} + \mathrm{C_A C_B}\ , \qquad (1)$$

where *E* and *C* constants (termed Drago constant below) are related to the electrostatic and covalent contributions to the acid-base interaction, and the subscripts *A* and *B* refer to the acidic and basic components, respectively.

Drago and co-workers determined the E and C constants for 40 acids and 40 bases. Therefore, Eq. (1) can be used, for any combination of acids and bases of known *E* and *C* constant, to predict the heats of adsorption. Thus, one very important use of *E* and *C* constants is the calculation of the heats of interaction for systems which have not been examined experimentally.

The *C*/*E* ratio gives a quantitative order of relative *hardness* or *softness* for the various Lewis acid-base sites and agrees well with the qualitative classification of Pearson [3]. Hard acids and bases have low ratios of *C*/*E*, and soft acids and bases have high ratios of *C*/*E*. Thus *C*/*E* ratios for acids are: 0.1 for hydrogen, 1.0 for iodine and for bases: 2 for aromatics ($\pi$-electrons), 6–11 for amines, and 20 for sulfur bases. Since the heats of adsorption from dilute solution are due to molecular interactions at interfaces, they can be correlated by the Drago constant according to Eq. (1). The heats of adsorption for systems which have not been examined experimentally can be predicted after the *E* and *C* constants are determined for the acidic and basic adsorption sites of the polymer interfaces.

This paper is concerned with the comparative analysis of surface properties of polymers where acid-base interactions determine, as a first approximation, the energy of adsorption. The heats of adsorption for the planar and particulate polymer surfaces were determined by calorimetric, ellipsometric, and contact angle techniques. The techniques of ellipsometry and adsorption-contact angle are applicable only to quasi-flat, extended surfaces, while that of calorimetry requires a solid material of high specific surface area. The acid and base properties of polymers were approximately estimated by using the Drago *E* and *C* constants.

## Experimental methods and instrumentals

### Calorimetry

Flow microcalorimetry is usually applied to determine the heats of adsorption from solutions of finely-divided powders. This method, including the flow diagram and block for the microcalorimetric experimental arrangement, was described in detail by Fowkes [4]. In our case, the flow microcalorimetry (Microscal Ltd., London, U.K.) has a 6-mm adsorption bed which is enclosed between inlet and outlet tubes, as shown in Fig. 1. The bed temperature is measured by two thermistors in the block which are in a Whetstone bridge circuit. The efficiency of the calorimeter depends on the degree of filling of the bed and the concentration adsorbate. In our case the maximum efficiency was found in the range of 50–120 mg of absorbents. The concentration of species in cyclohexane solutions was determined by UV absorption with a Perkin-Elmer Lambda V spectrometer operating in the Beer's law region. Adsorption exotherms and UV absorption plots in this paper were measured at 23 °C; the molar heats of adsorption were determined form this data, according to the well-known method [4] of flow microcalorimetry. The standard deviations in the heats of adsorption in repeat runs were found to be about 5% in all cases.

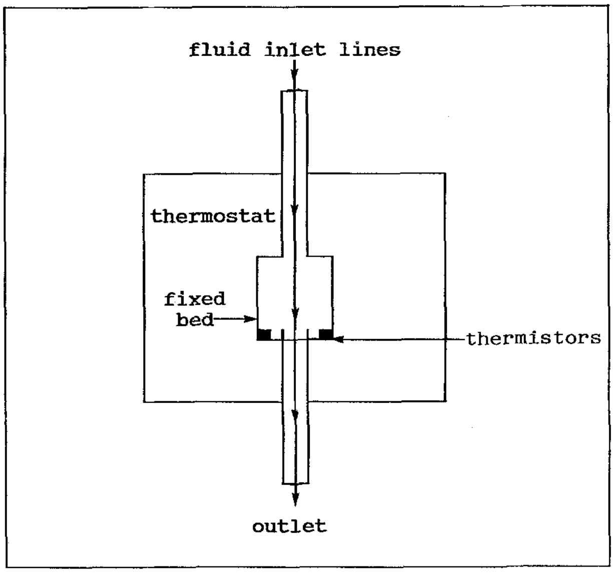

Fig. 1. Flow calorimetry cell for the microcalorimetric experimental measurement of the heat of adsorption

### Contact angles

The method of contact angle titration makes it possible to directly determine [5, 6] the surface concentrations and strengths of acidic and basic surface sites on a microscopically flat surface of the polymer film. To study the acid-base properties of polymer films, dilute solutions of phenol and THF in methylene iodide were chosen respectively. Since methylene iodide ($CH_2I_2$) is a van der Waals liquid having high surface tension, it forms finite contact angles on most polymer surfaces. The surface tension of the solutions was found by the drop volume technique [7]. The contact angles were measured using a Rame-Hart contact angle goniometer with a covered chamber for viewing the drops. The average diameters of drops on the plane of films was 2.5–3 mm.

Let us consider the method calculating the heats of adsorption and parameters of adsorption isotherms by using measurements of contact angles on the flat surfaces.

The number of sites per unit area of the polymer film can be determined by an analysis based on the combination of Gibbs adsorption (Eq. (2)) with Young's (Eq. (3)) and the Langmuir adsorption isotherm (Eq. (4)): Gibbs adsorption equation may be written

$$\Gamma = -(c/RT)\,\partial(\gamma_{SL})/\partial c\,, \tag{2}$$

where *c* is the adsorbate concentration in solution, *R* is the universal gas constant, *T* is the absolute temperature, $\gamma_{SL}$ is the surface tension onto the solid-liquid surface, Young's equation may be written

$$\gamma_{SL} = \gamma_{SL} - \gamma_{LV}\cos\theta\,, \tag{3}$$

where $\gamma_{SV}$ is the surface tension onto the solid-vapor surface, $\gamma_L$ is the surface tension of the liquid-vapor surface, and $\Theta$ is the contact angle.

The Langmuir adsorption isotherm equation may be written

$$\Gamma = \Gamma_m K_p c/(1 + K_p c) , \quad (4)$$

where $\Gamma$ is the adsorbate concentration per unit surface area, $\Gamma_m$ is the maximum adsorbate coverage, $K_p$ is the equilibrium constant.

Inserting Eq. (3) into Eq. (2) gives

$$\Gamma = (c/RT)\, \partial(\gamma_L \cos\Theta)/\partial c . \quad (5)$$

Assuming as a first approximation that the adsorption process is described by the Langmuir adsorption equation, Eq. (4) and Eq. (5) can be rearranged to give:

$$\partial(\gamma_L \cos\Theta)/\partial c = RT\Gamma_m K_p/(1 + K_p c) . \quad (6)$$

After integration Eq. (6) takes the form:

$$\gamma_L (\cos\Theta - \cos\Theta_0) = RT\Gamma_m \ln(1 + K_p c) . \quad (7)$$

For the relative small concentrations of adsorbate [8], Eq. (7) can be reduced to:

$$\gamma_L \cos\Theta = \gamma_L \cos\Theta_0 + RT\Gamma_m [(K_p c) - (K_p c)^2/22 + (K_p c)^3/3] . \quad (8)$$

In this case the experimental dependence of $[\gamma_L (\cos\Theta)]$ on concentration, $c$, can be treated by using a computer fit which can be described as

$$\gamma_L \cos\Theta = a_0 + a_1 c - a_2 c^2 + a_3 c^3 \quad (9)$$

$$a_0 = \gamma_L \cos\Theta_0,\ a_1 = RT\,\Gamma_m\, K_p,$$
$$a_2 = RT\,\Gamma_m\, K_p^2/2, \quad a_3 = RT\,\Gamma_m\, K_p^3/3 . \quad (10)$$

The coefficients of the Langmuir adsorption isotherm from Eqs. (9) and (10) is given by

$$K_p = 2a_2/a_1, \quad \Gamma_m = a_1^2/(2RTa_2) . \quad (11)$$

If the dimension of $\gamma_L$ is dynes/cm and the concentration of $c$ is mol/m$^3$ (or [mmol/L]), then

$$\Gamma_m(T)\,[\mu\text{mol/m}^2] \approx 0.2(T_0/T)\,(a_1^2/a_2),$$
$$T_0 = 296\,°\text{K},\ K_p\,[\text{mmol/L}] = 2a_2/a_1 . \quad (12)$$

In the case of Eq. (9) the coefficient of $a_3$ may be used as a criterion to apply the Langmuir adsorption isotherm. As according to Eq. (10), it is reasonable to write

$$\delta° = |1 - 3a_1 a_3/(4a_2^2)| . \quad (13)$$

The value of $\delta°$ is equal to zero when the Langmuir adsorption isotherms are valid. The estimations have shown that Eqs. (10) through (13) are reasonable to use for the calculation of values $K_p$ and $\Gamma_m$ from the experimental data when the value of $\delta°$ is no more than 0.5. Otherwise, the error in calculating $K_p$ and $\Gamma_m$ increases when the value of $\delta°$ increases.

The Langmuir isotherm equation allows one to determine the equilibrium constant, $K_p$, by the heats of adsorption calculated from the van't Hoff [9] equation, if the values of $K_p$ are determined at two temperatures

$$\Delta H^{ab} = [RT_1T_2/(T_1 - T_2)]\ln \times [K_p(T_1)/K_p(T_2)] \quad (14)$$

### *Ellipsometry*

Ellipsometry is a sensitive and non-destructive method for measuring the thickness of thin films at the interface [10–12], since the film changes the state of polarization of an incident light beam upto reflection from the interface. Ellipsometric measurements are only feasible for microscopically flat surfaces. The sensitivity of this method depends on the differences in refractive index between the adsorption layer and solution. Therefore, reliable measurements can only be obtained if the refractive index of the adsorption layer is higher than that of the solution.

We consider two groups of techniques for the measurement of adsorption isotherms and the heat of adsorption: static (equilibrium) and kinetic (non-equilibrium) methods.

Several authors have used ellipsometry to measure the adsorption layer thickness at the interface [10] (adsorption equilibrium, i.e., static method). On the other hand, ellipsometry makes it possible to measure adsorption processes continuously with time (non-equilibrium adsorption, i.e., kinetic method). This method was applied in this paper. Kinetic measurements are typically of a non-equilibrium nature, since the adsorbate thickness is inferred from the outward displacement of *probe-molecules* due to the adsorbate of the slipping layer between the solid and liquid phase. In fact, an adsorbed layer is clearly not homogeneous, but its concentration is a continuously decreasing function with increasing distance from the surface. Therefore, the thickness found from the ellipsometric kinetic measurements, by considering the adsorption layer as a quasi-homogeneous film of constant local concentration, is an average.

The equilibrium adsorption of phenol from cyclohexane on polyimide/siloxane and 6F photoimagable fluorinated polyimide films and adsorption kinetics at the interface have been investigated by ellipsometry. Details of ellipsometric method are discussed in the Appendix A. Complex samples consisting of three of the uniform parallel films are shown in Fig. 2. From the system of Eqs. (A10) the values of $n_j$ and $k_j$ or the values of $d_j$ and $n_j$ can be calculated successively. First, the $SiO_2$-Si water thickness, $d_3$, is determined, then the $SiO_2$-Si-(polymer film) wafer thickness of polymer film, $d_2$, is calculated.

Adsorption studies were performed in a custom glass cell, as is shown in Fig. 3. The values of $d_3$ and $d_2$ are found in air without the cell. The thickness of the adsorption layer, $d_1$, is determined by using the Eq. (A10). Complications are encountered in calculating adsorption layers and film thickness. In fact, there exists a thickness of $d_0$ in which the polarization change is 360°. For example, the thickness of $d_0$ is 281.5 nm for the $SiO_2$ layer on silicon measured using a He/Ne laser, $\lambda = 632.8$ nm, and an incident angle of 70°. The layers, having thicknesses of $d = (d_1^0 + nd_0)$, $n = 1,2,3,\ldots$, all have the same $\Delta$ and $\psi$ values. Therefore, it is necessary to use the films having the thicknesses less then $d_0$, i.e., $d < d_0$.

Now, we consider the adsorption layers. Strictly speaking, the concentration-adsorption profile (in the directional normal to the film surface) is variable, and we measure the *apparent* adsorption layer thickness average with respect to the normal concentration profile. As shown in the Appendix B, the Gibbs surface excess, $\Gamma$, is therefore given by

$$\Gamma = d_{\text{adsorbate}}\rho_{\text{adsorbate}}X_{\text{adsorbate}}/M_{\text{adsorbate}} , \quad (15)$$

where $\Gamma$ is the adsorbate concentration per unit surface area; $d_{\text{adsorbate}}$ is an *apparent* thickness of the adsorption layer; $\rho_{\text{adsorbate}}$ is the adsorbate density; $X_{\text{adsorbate}}$ is the weight fraction of adsorbate in the adsorption layer; $M_{\text{adsorbate}}$ is the adsorbate molecular weight.

The value of the weight fraction $X_{\text{adsorbate}}$ may be found from the Lorentz-Lorenz equation written in the form of Eq. (B12).

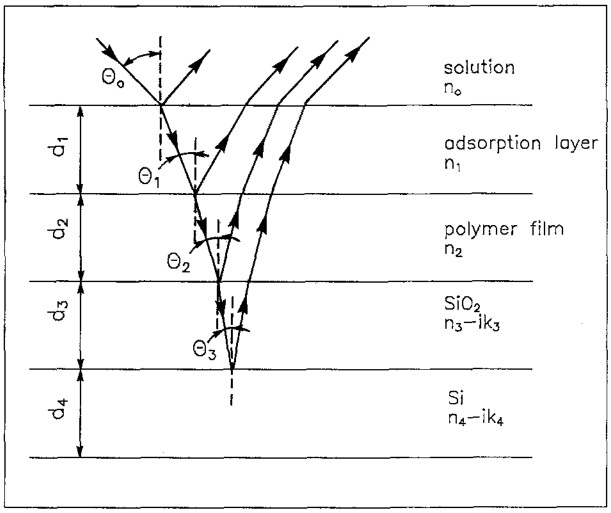

Fig. 2. Optical model of a symmetrical three-layer film

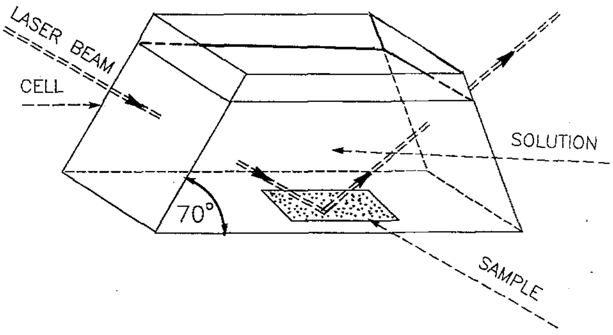

Fig. 3. Cell for the ellipsometric experimental arrangement

The equilibrium adsorption data were analyzed by the Langmuir adsorption isotherm Eq. (4). In most cases adsorption equilibrium on polymer surfaces [14, 15] is described by Langmuir adsorption isotherms only for relative small concentrations of adsorbate. Therefore, according to Eqs. (4) and (9), it is reasonable [8], for relative small adsorbate concentrations, to determine the experimental, $\Gamma_{\text{exp}}$, and calculated, $\Gamma_{\text{cal}}$, values of adsorption isotherms as

$$\Gamma_{\text{exp}} = b_1c - b_2c^2 + b_3c^3$$

$$\Gamma_{\text{cal}} = \Gamma_m[K_pc - (K_pc)^2 + (K_pc)^3] .$$

The coefficients in Eq. (16) are given by

$$b_1 = \Gamma_m K_p, b_2 = \Gamma_m K_p^2, b_3 = \Gamma_m K_p^3,$$

$$K_p = b_2/b_1, \quad \Gamma_m = b_1^2/b_2 . \quad (16)$$

If the dimension of $\Gamma_{\mathrm{exp}}$ is $\mu$mol/m$^2$ and the concentration of $c$ is mmol/L, then

$$K_{\mathrm{p}}[\mathrm{L/mmol}] = b_2/b_1, \Gamma_{\mathrm{cal}}[\mu\mathrm{mol/m^2}] = b_1^2/b_2 \quad (17)$$

In Eq. (16) the coefficients of $b_3$ may be used as a criterion to apply the Langmuir adsorption isotherms in Eq. (4). According to Eq. (17), it is reasonable to write

$$\delta^* = |1 - b_1 b_3/b_2^2| \,. \quad (18)$$

The value of $\delta^*$ is equal to zero when the Langmuir adsorption isotherms are valid.

Now, we consider the method based on an analysis of adsorption kinetics. The local adsorption equilibrium at the interface is reached in a dynamic way, because the adsorption process on the polymer/solution interface is governed by diffusion [8, 16–19]. According to the analysis [8, 16–19], the adsorption process as $t \to 0$ can be described in the following form

$$\Gamma_{\mathrm{rel}} = \Gamma/\Gamma_0 \approx a_0^0(c_0/\Gamma_0)t^{1/2} \,, \quad (19)$$

where $\Gamma_0$ is the maximum amount of adsorption (dependent on the adsorbate concentration in solution).

For different temperatures, the time dependence of $\Gamma_{\mathrm{rel}}$ versus $t^{1/2}$ is linear for short time periods. According to Eq. (19), for the Langmuir adsorption isotherm the slope, $s_0$, is given as

$$s_0 = a_0(1+b)/b, \mathrm{b} = K_{\mathrm{p}}^*\mathrm{c}, K_{\mathrm{p}}^*(T)$$
$$= K_{\mathrm{p}}^0 \exp(\Delta H_0^{*\mathrm{ab}}/RT), a_0 = \mathrm{constant}\,, \quad (20)$$

where $(-\Delta H_0^{*\mathrm{ab}})$ is the apparent activation energy of the non-equilibrium adsorption process on the polymer/solution interface as $t \to 0$.

According to the van't Hoff equation [9] and Eq. (20), the apparent activation energy of the adsorption process, $(-\Delta H_0^{*\mathrm{ab}})$, may be calculated by using Eq. (24) if the value of $b(T_1)$ is found from the equilibrium measurement at temperature $T_1$ and the values of slope, $s_0(T_1)$ and $s_0(T_2)$, obtained from the kinetic measurements at temperatures $T_1$ and $T_2$, respectively,

$$\Delta H_0^{*\mathrm{ab}} = R[T_1T_2/(T_2 - T_1)]\ln\{1 + [1 + b(T_1)]$$
$$\times(\alpha_0 - 1)\}, \alpha_0 = s_0(T_1)/s_0(T_2)\,. \quad (21)$$

The adsorption process as $t \to \infty$ can be described in the following form [8, 16–19]

$$\Gamma_{\mathrm{rel}} \approx 1 - a_\infty^0[d\Gamma(c_0)/dc]t^{-1/2},$$
$$d(1 - \Gamma_{\mathrm{rel}})/dt^{-1/2} \approx a_\infty^0[d\Gamma(c_0)/dc]\,. \quad (22)$$

For different temperatures, the time dependence of $(1 - \Gamma_{\mathrm{rel}})$ versus $t^{-1/2}$ is linear for long time period. According to Eq. (22), for the Langmuir adsorption isotherm the slope, $s_\infty$, is given by

$$s_\infty = a_\infty b/(1+b)^2, b = K_{\mathrm{p}}^*\mathrm{c}, K_{\mathrm{p}}^*(T)$$
$$= K_{\mathrm{p}}^0 \exp(\Delta H_\infty^{*\mathrm{ab}}/RT), a_\infty = \mathrm{constant}\,, \quad (23)$$

where $(-\Delta H_\infty^{*\mathrm{ab}})$ is the apparent activation energy of the non-equilibrium adsorption process on the polymer/solution interface as $t \to \infty$.

According to the van't Hoff equation [9] and Eq. (23), the apparent activation energy of the adsorption process, $(-\Delta H_\infty^{*\mathrm{ab}})$, may be calculated by using Eq. (24) if the value of $b(T_1)$ is found from the equilibrium measurement at temperature $T_1$ and the values of slope, $s_\infty(T_1)$ and $s_\infty(T_1)$, obtained from the kinetic measurements at temperatures $T_1$ and $T_2$, respectively,

$$\Delta H_\infty^{*\mathrm{ab}} = -R[T_1T_2/(T_2 - T_1)]$$
$$\times \ln[B - (B^2 - b_1^{-2})^{1/2}],$$
$$B = [\alpha_\infty(1+b_1)^2 - 2b_1]/(2b_1^2)$$
$$b_1 = b(T_1), \quad \alpha_\infty = s_\infty(T_1)/s_\infty(T_2) \quad (24)$$

Thus, the apparent activation energy of the adsorption process can be calculated from Eqs. (21) and (24) by using the experimental kinetic data.

Ellipsometry measurements were performed with a Rudolph Auto El ellipsometer, using a He/Ne laser, $\lambda = 632.8$ nm, and an incident angle of 70 °. A stress-free cell with faces set at 70.0 ° (Precision Cells, Inc.) was utilized for the adsorption measurements, as shown in Fig. 3. Solvent was placed over the sample in the cell and stable base values of $\Delta$ and $\psi$ were established for a period of 1–2 min. Phenol solution was then introduced into the cell, and the ellipsometric parameters $\Delta$ and $\psi$ were then monitored every 15–20 s.

## Experimental materials

The polyimide/siloxane [poly(imide/siloxane) block copolymers (siloxane 35%) with a molecular weight of 960], 6F photoimagable fluorinated polyimide (with a molecular weight of 720) and 6F polyimide (with a molecular weight of 690) were investigated. Cyclohexane was dried with 10 mesh Davison 3-Å molecular sieves. Solutions were made fresh daily. The organic bases used for titration of surface activity included pyridine (99 + % mole pure, Aldrich chemical), ethyl acetate (certified ACS grade from Fisher Scientific), chloroform (99.9 + %, A.C.S. HPLC grade), iodine and dimethyl sulfide (99 + %, Aldrich Chemical). The phenol was purchased from Aldrich and sublimed before use. The methylene iodine 99%, was purchased from Aldrich and purified before use by passing through a column of basic alumina; the resulting liquid was a pale straw color; all solutions for titrations by contact angels were stabilized with copper turnings and stored in the dark. The thicknesses of polymer films (spin-coated onto 10-cm polished silicon wafers) used in these studied were 80, 100, 120 nm for polyimide/siloxane, 6F photoimagable fluorinated polyimide, 6F polyimide, respectively. Most measurement were made at 23 °C and in a 10 °C coldroom in which the solutions and apparatus were stored overnight before measurements were made.

## Discussion

The heats of adsorption for the various types of polymer powders were measured by flow microcalorimetry [4]. The values are listed in Table 1. The statistical analysis of the flow microcalorimetric measurements shows that the standard deviations in the heats of adsorption in Table 1 in repeat runs were found to be about 5% in all cases.

Three Lewis acids (phenol, chloroform, and iodine) and three Lewis bases (pyridine, ethyl acetate, and dimethyl sulfide) were used as *probe* molecules with the known Drago constant [1, 2, 4] for the estimation of acidity-basicity properties of sites on the substrate and polymeric solids. According to references [1, 2, 4], the values of the Drago constants may be found graphically.

The $E_A$, $E_B$ and $C_A$, $C_A$ constants for the surface sites of polymer films have been determined calorimetrically from the heats of adsorption of acidic or basic test probe molecules of known $E_A$, $E_B$ and $C_A$, $C_A$ constants, as illustrated in Figs. 4–6. These figures is a graphical method of solving two and three equations for two unknowns ($E_A$ and $C_A$ or $E_B$ and $C_B$). In these figures, each straight line represents the average heat of adsorption of a test base or acid with the surface sites of a fine polymer powder, using the Drago Eq. (1) in the following forms

$$E_A = (-\Delta H^{ab})/E_B - C_A(C_B/E_B),$$

$$E_B = (-\Delta H^{ab})/E_A - C_B(C_A/E_A)\ .$$

The intercept at $C_A = 0$ is $(-\Delta H^{ab})/E_B$, and the slope is $C_B/E_B$. The intercept at $C_B = 0$ is $(-\Delta H^{ab})/E_A$, and the slope is $C_A/E_A$. In Figs. 4–6 it can be seen that the test bases were

Table 1. Heat of Adsorption by Microcalorimetry (kJ/mol)

| | Powder Polymer | | |
|---|---|---|---|
| | polyimide/ siloxane | 6F photo-imagable fluorinated polyimide | 6F polyimide |
| Phenol | 50.78 | 58.88 | 42.6 |
| Chloroform | 26.1 | 29.38 | 13.44 |
| Iodine | 14.0 | 21.6 | 13.1 |
| Dimethyl sulfide | 25.2 | 25.97 | 10.22 |
| Ethyl acetate | 12.5 | 22.44 | 9.68 |
| Pyridine | 25.66 | 41.18 | 17.65 |

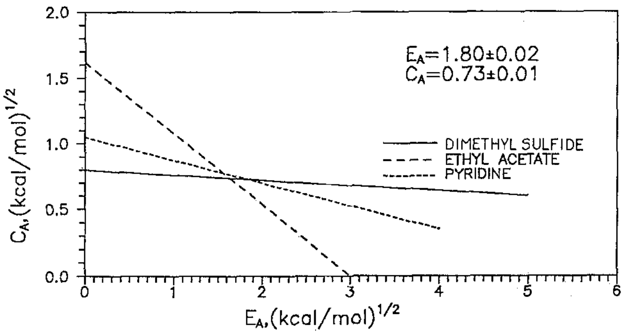

Fig. 4. Graphical determination of the *E* and *C* parameters for polyimide/siloxane powder using the heat of adsorption by microcalorimetry as listed in Table 1

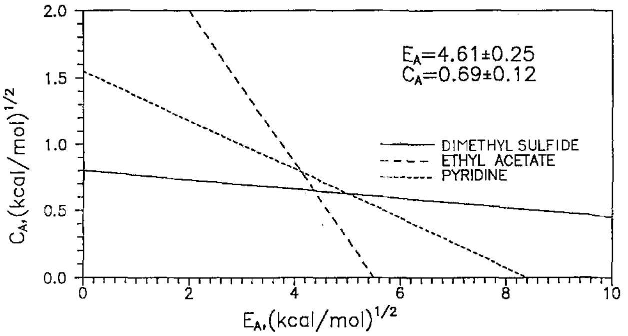

Fig. 5. Graphical determination of the $E$ and $C$ parameters for 6F photoimagible fluorinated polyimide powder using the heat of adsorption by microcalorimetry as listed in Table 1

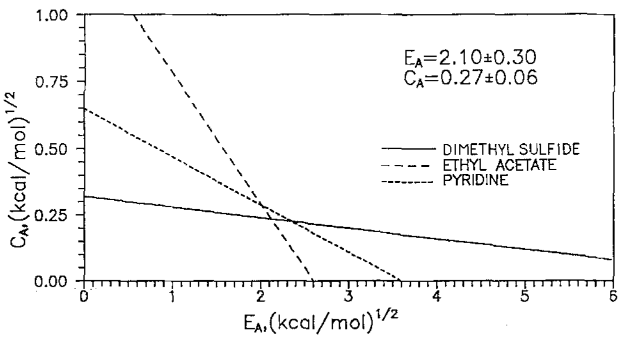

Fig. 6. Graphical determination of the $E$ and $C$ parameters for 6F polyimide powder using the heat of adsorption by microcalorimetry as listed in Table 1.

Table 2. Drago $E$ and $C$ Constants for Powder Polymer [units of (kcal/mol)$^{1/2}$]

| | Powder Polymer | | |
|---|---|---|---|
| | polyimide/ siloxane | 6F photoimagable fluorinated polyimide | 6F polyimide |
| $C_B$ | 1.03 | 2.75 | 1.5 |
| $E_B$ | 2.34 | 2.63 | 1.6 |
| $C_B/E_B$ | 0.44 | 1.04 | 0.93 |
| $C_A$ | 0.73 | 0.69 | 0.27 |
| $E_A$ | 1.8 | 4.61 | 2.1 |
| $C_A/E_A$ | 0.4 | 0.15 | 0.13 |

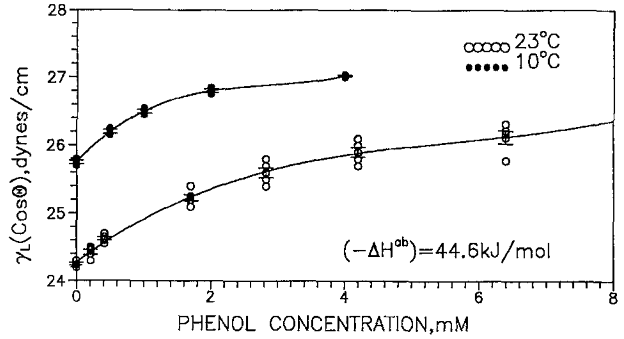

Fig. 7. Gibbs plot of the decrease in interfacial free energy at the solution-polyimide/siloxane interface ($\gamma_L$Cos$\Theta$) versus phenol concentration in $CH_2I_2$

chosen to have different $C_B/E_B$ slopes so as to have statistically significant intersections because the $E_A$ and $C_A$ constants for polymer films are determined from the intersection.

The data are plotted in the form of graphical solutions of the Drago Eq. (1) for the three substrate materials and the various polymers (polyimide/siloxane, 6F photoimagible fluorinated polyimide and 6F polyimide), as shown in Figs. 4–6, respectively. The resulting Drago constants for the various polymers are summarized in Table 2.

From Table 2 it follows that the basic constants show that the polyimide/siloxane is of intermediate strength and is significantly harder than 6F photoimagible fluorinated polyimide and 6F polyimide. The acidic constants show that the polyimide/siloxane is significantly softer than 6F photoimagible fluorinated polyimide and 6F polyimide.

Calorimetric techniques used for powder and fiber analysis are not sensitive enough for such a flat surface as polymer films.

A contact angle technique allows one direct determination of the surface tension, $\gamma_L\cos\Theta$, on the solution-solid interface if the surface is microscopically flat.

In this study methylene iodine ($CH_2I_2$) has been used as the solvent, since this liquid has a high surface tension and large contact angles for most polymers.

The experimental dependencies ($\gamma_L$ $\cos\Theta$) versus phenol concentration, $c$, for two temperatures are shown in Fig. 7 for the series of phenol-methylene iodine solutions onto polyimide/siloxane. Since contact angles decrease with time, all measurements were made after waiting 1h, when changes of contact angles were negligible. The data points between 0 (pure solution) and 6.4 mM at 23 °C and the data between 0 and 4 mM at 10 °C data were fit to third-order polynomial functions. By use of a computer with these experimental data, Eq. (9) can be found in the following form

$$\gamma_L(\cos\Theta) = 24.28 + 0.73c - 0.11c^2 + 0.0065c^3 \text{ (at 23 °C)}$$

$$\gamma_L(\cos\Theta) = 25.71 + 1.16c - 0.403c^2 + 0.0485c^3 \text{ (at 10 °C)} .$$

From the preceding equations and by using Eqs. (12) and (13), we find the constants $K_p = 0.301$L/mmol, $\delta^\circ = 0.7$ (at 23 °C), $K_p = 0.695$L/mmol, $\delta^\circ = 0.74$ (at 10 °C) and heat of adsorption

$$(-\Delta H^{ab}) = 53.55 \ln[K_p(T_1)/K_p(T_2)] = 44.6 \text{ kJ/mol} .$$

For the preceding case, the accuracy of the calculation of the heat of adsorption is relatively slow, since, according to Eqs. (9)–(13), the accuracy of calculations decreases when the value of $\delta^\circ$ is more than 0.5.

It should be noted that in some cases the values of contact angles change minimally when adsorbate concentrations increase significantly. For example, the contact angles scarcely changed when phenol concentrations were more than 4 mM at 10 °C and more than 7 mM at 23 °C for polyimide/siloxane films. For 6F photoimagable fluorinated polyimide and 6F polyimide films, the change of contact angles, depending on phenol concentrations, was negligible; therefore, in these cases the contact angle technique is ineffective. This difficulty may be surmounted by using ellipsometry.

An ellipsometric technique allows one to directly determine the adsorption layers on polymer films when solutions have arbitrary values of both surface tensions and contact angles.

The equilibrium adsorption of phenol in cyclohexane on polyimide/siloxane, 6F photoimagible fluorinated polyimide and 6F polyimide films has been investigated by ellipsometry.

Gibbs adsorption isotherms for phenol in cyclohexane on the various polymer films at 23 °C and 10 °C are presented in Figs. 8–10, respectively. From the experimental data in Figs. 8–10 and Eqs. (16), adsorption parameters and heat of adsorption are equal to:

for polyimide/siloxane

$$\Gamma_m = 1.91\ \mu\text{mol/m}^2,\ K_p = 0.031\text{L/mmol(23 °C)},$$

$$\delta^* = 0.23\text{(23 °C)}$$

$$K_p = 0.0715\text{L/mmol(10 °C)},\ \delta^* = 0.16\text{ (10 °C)},$$

$$(-\Delta H^{ab}) = 44.7\text{ kJ/mol}$$

for 6F photoimagible fluorinated polyimide

$$\Gamma_m = 4.05\ \mu\text{mol/m}^2,$$

$$K_p = 0.044\text{L/mmol(23 °C)},$$

$$\delta^* = 0.13\text{(23 °C)},$$

$$K_p = 0.111\text{L/mmol(10 °C)};\ \delta^* = 0.15\text{ (10 °C)},$$

$$(-\Delta H^{ab}) = 49.5\text{ kJ/mol}$$

for 6F polyimide

$$\Gamma_m = 1.24\ \mu\text{mol/m}^2,\ K_p = 0.0297\text{L/mmol(23 °C)},$$

$$\delta^* = 0.3\text{(23 °C)},$$

$$K_p = 0.0598\text{L/mmol(10 °C)},\ \delta^* = 0.24\text{ (10 °C)},$$

$$(-\Delta H^{ab}) = 37.5\text{ kJ/mol} .$$

For the preceding cases the accuracy of the calculations of the heats of adsorption is relatively high, since, according to Eqs. (16) and (18), the

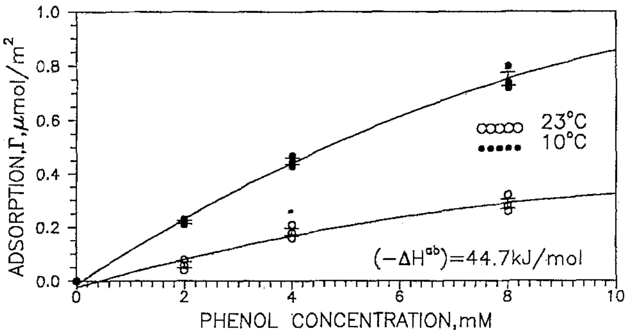

Fig. 8. Adsorption isotherms for phenol from cyclohexane on polyimide/siloxane film for different temperatures

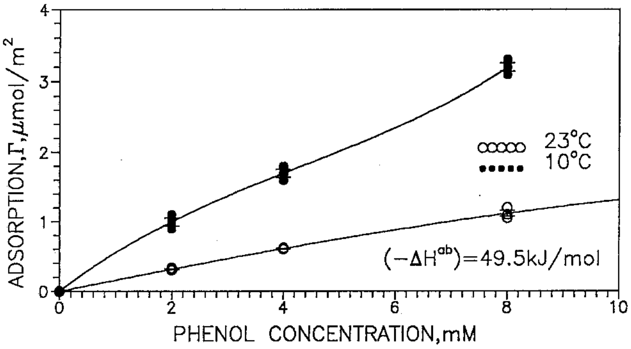

Fig. 9. Adsorption isotherms for phenol from cyclohexane on 6F photoimagible fluorinated polyimide film for the different temperatures

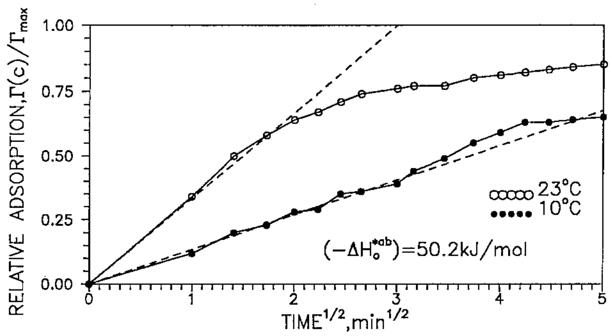

Fig. 11. Relative adsorption versus $t^{1/2}$ for phenol from cyclohexane on polyimide/siloxane film for the different temperatures

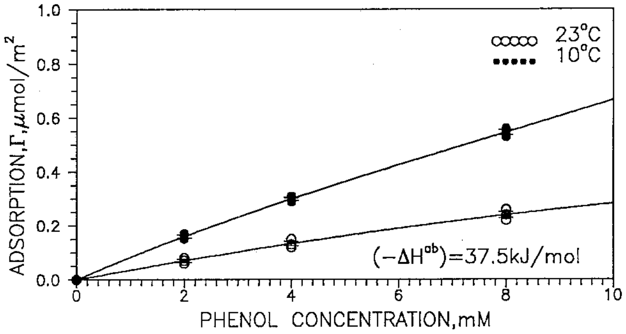

Fig. 10. Adsorption isotherms for phenol from cyclohexane on 6F polyimide film for different temperatures

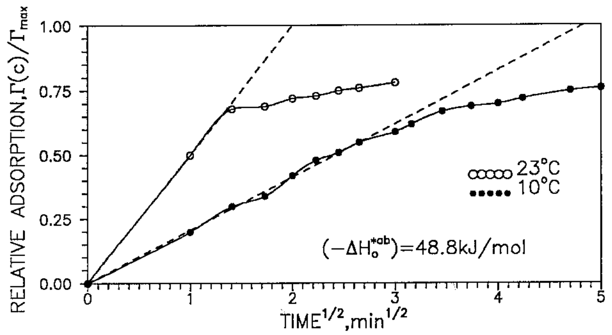

Fig. 12. Relative adsorption versus $t^{1/2}$ for phenol from cyclohexane on photoimagible fluorinated polyimide film for the different temperatures

accuracy of calculations decreases when the value of $\delta^*$ is more than 0.5.

It should be noted that the foregoing values of the heat of adsorption are averaged values with respect to the phenol concentrations.

The non-equilibrium adsorption of phenol in cyclohexane on polyimide/siloxane, 6F photoimagible fluorinated polyimide and 6F polyimide films has been investigated by ellipsometry.

The kinetics curves for adsorption of 2 mM phenol in cyclohexane on the various films at 23 °C and 10 °C are presented in Figs. 11–14. As shown in Figs. 11 and 12, for the two temperatures, $\Gamma_{\mathrm{rel}}$ versus $t^{1/2}$ are the straight lines as $t \to 0$. Inserting the values of the slopes, $s_0$, at temperatures $T_1$ and $T_2$ into Eq. (21), the apparent activation energy of the adsorption process is $(-\Delta H_0^{*\mathrm{ab}}) = 50.2$ kJ/mol for polyimide/siloxane and $(-\Delta H_0^{*\mathrm{ab}}) = 48.8$ kJ/mol for 6F photoimagible fluorinated polyimide. Similarly, as shown in Figs. 13 and 14, $-ln(1-\Gamma_{\mathrm{rel}})$ versus $t^{-1/2}$ are the straight lines as $t \to \infty$. Inserting the values of the slopes, $s_\infty$, at temperatures $T_1$ and $T_2$ into Eq. (24), the apparent activation energy of the adsorption process are $(-\Delta H_0^{*\mathrm{ab}}) = 52.7$ kJ/mol for polyimide/siloxane and $(-\Delta H_0^{*\mathrm{ab}}) = 46.7$ kJ/mol for 6F photoimagible fluorinated polyimide.

The values of effective heat of adsorption obtained from the asymptotic analysis is kinetic curves as $t \to 0$ and $t \to \infty$ are almost identical. The standard deviations in the heats of adsorption in repeat runs obtained from the ellipsometric data were found to be about 7% in all cases.

Thus, the method based on the asymptotic analysis of kinetics curves allows one to measure on planar polymer surfaces the apparent activation energy over a wide range of adsorbate concentrations. Therefore, the ellipsometric kinetic method

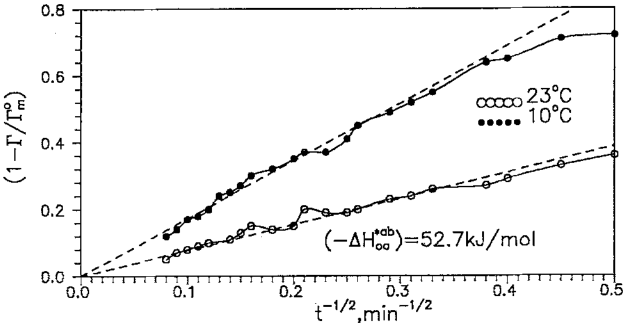

Fig. 13. -ln(1-Relative adsorption) versus $t$ for phenol from cyclohexane on polyimide/siloxane film for the different temperatures

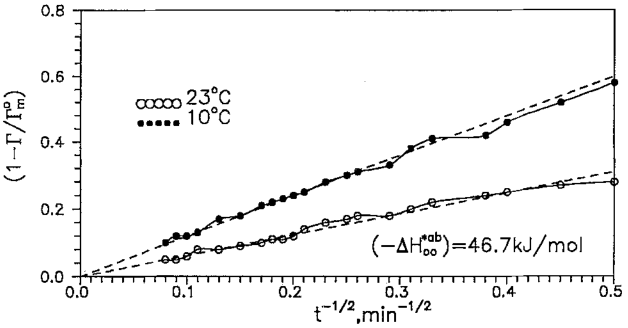

Fig. 14. -ln(1-Relative adsorption) versus $t$ for phenol from cyclohexane on photoimagible fluorinated polyimide film for the different temperatures

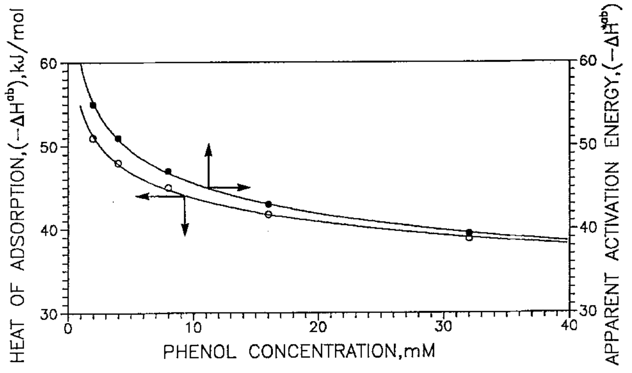

Fig. 15. Apparent activation energies of the adsorption process and heats of adsorption on polyimide/siloxane film versus for phenol concentrations

can be used to directly study the non-equilibrium adsorption processes on planar polymer surfaces.

Now let us compare the heats of adsorption ( $-\Delta H^{ab}$), obtained by ellipsometry for the equilibrium case, with the apparent activation energy of the adsorption processes ( $-\Delta H^{*ab}$), obtained by ellipsometry for the non-equilibrium (kinetic) case. The apparent activation energies of the adsorption process ( $-\Delta H^{*ab}$), on polyimide/siloxane film from cyclohexane over a wide range of phenol concentrations in cyclohexane, measured by ellipsometry in the non-equilibrium (kinetic) case, and the heats of adsorption ( $-\Delta H^{ab}$), obtained by ellipsometry for the equilibrium case, are represented in Fig. 15. The values of both ( $-\Delta H^{*ab}$) and ( $-\Delta H^{ab}$) decrease with occupation of the active sites of the polymer films.

The heats of adsorption phenol from cyclohexane on polyimide/siloxane film calculated from the adsorption isotherms for the temperatures are presented in Figs. 8–10. From the analysis of these results shown in Figs. 8, 9 and 15, it follows that the values of the heats of adsorption, obtained from Figs. 8 and 9 (in fact, averaged over the adsorbate concentrations), are nearly coincident with the values of apparent activation energies of the adsorption process determined from Fig. 15 after averaging with respect to phenol concentrations, From the preceding results it follows that values of the heats of adsorption on polymer powders and polymer films obtained by flow microcalorimetric, contact angle, and ellipsometric techniques have given good congruent results.

## Conclusions

The heats of adsorption on a planar surface (polymer films) and a particular surface (polymer powders) and polyimide/siloxane, 6F photoimagible fluorinated polyimide and 6F polyimide obtained by using various techniques (flow microcalorimetry, contact angle and ellipsometry) are found to be approximately the same. The Drago acid and base constants calculated for various polymers allow us to estimate the softness and hardness of acid-base sites of polyimide/siloxane, 6F photoimagible fluorinated polyimide and 6F polyimide by using the values of ratios of $C/E$ represented in Table 2.

The method of analysis of acidic-basic properties, based on the use of adsorption kinetic curves obtained by ellipsometry, have essential advantages over the contact angle technique. Therefore, this method may be used for the investigation of the interface of polymer films.

## Appendix A

The optical system used, as shown in Fig. 2, consists of the following layers: bulk silicon (Si) with a complex refractive index, $n^* = n_4 - ik_4$, a layer of silica ($SiO_2$) with a refractive index $n_3$ with a thickness $d_3$, the polymer film with the refractive index $n_2$ and a thickness $d_2$, the adsorbed layer with a refractive index $n_1 = n_{\mathrm{ad.layer}}$ and a thickness $d_1 = n_{\mathrm{ad.layer}}$, and a surrounding solution with the refractive index $n_0$.

The state of polarization of polarized light is changed upon reflection at a surface. The total electric vector $E$ may be resolved normal to the plane of incident and both normal to the direction propagation, i.e., $E_p^{(i)}$, $E_p^{(r)}$ and $E_s^{(i)}$, $E_s^{(i)}$, where the superscripts $(i)$ and $(r)$ correspond to the incident and reflected waves, respectively.

The overall reflection coefficients for the normal ($R^{(p)}$) and perpendicular ($R^{(s)}$) polarized light for the multilayer film are given by [13]

$$R^{(x)} = [r_{01}^{(x)} + R_{12}^{(x)} \exp(-2i\delta_1)]/[1 + r_{01}^{(x)} R_{12}^{(x)} \times \exp(-2i\delta_1)],\ i = (-1)^{1/2} \tag{A1}$$

$$R_{j(j+1)}^{(x)} = [r_{j(j+1)}^{(x)} + R_{(j+1)(j+2)}^{(x)} \exp(-2i\delta_j)]/ \times [1 + r_{j(j+1)}^{(x)} R_{j(j+1)(j+2)}^{(x)} \times \exp(-2i\delta_j)],\ j = 1, 2 \tag{A2}$$

$$\delta_k = (2\pi/\lambda) d_k \cos\theta_k,\ k = 1, 2, 3, \tag{A3}$$

where $(x)$ denotes the normal $(p)$ and perpendicular $(s)$ directions of the polarized light; $\delta_k$ is the phase shift in radians of the polarized light; The Fresnel reflection coefficients are given by

$$r_{j(j+1)}^{(p)} = (n_{(j+1)}^* \cos\theta_j - n_j^* \cos\theta_{(j+1)})/n_{(j+1)}^* \times \cos\theta_j + n_j^* \cos\theta_{(j+1)}),\ 0 \le j \le 3 \tag{A4}$$

$$r_{j(j+1)}^{(s)} = (n_j^* \cos\theta_j - n_{(j+1)}^* \cos\theta_{(j+1)})/(n_j^* \cos\theta_j + n_{(j+1)}^* \cos\theta_{(j+1)}),\ n_j^* = n_j - ik_j\ , \tag{A5}$$

where $j$ and $j+1$ are the subscripts of media $n_j^*$ and $n_{j+1}^*$, respectively; $n_j^*$ is a complex refractive index; $n_j$ and $k_j$ are real and imaginary components of the refractive index; $\theta_j$ and $\theta_{j+1}$ are the incident and reflection angles, respectively; $n_j$ is the refractive index of layer $j$ and $\theta_j$ is the incidence angle at layer $j$.

The refractive indices and the incidence angles at layers $j$ and $(j+1)$ are related to each other according to Snell's law

$$n_{(j+1)}^* \sin\theta_{(j+1)} = n_j^* \sin\theta_j,\ 0 \le j \le 3\ . \tag{A6}$$

The angles $\psi$ and $\Delta$ measured by ellipsometry are related to the reflection coefficients of the normal ($R^{(p)}$) and perpendicular ($R^{(s)}$) polarized light components by

$$\rho \equiv R^{(p)}/(R^{(s)} = \tan(\Psi)\exp(i\Delta) \tag{A7}$$

Let

$$\eta = \exp(-2i\delta_1)\ . \tag{A8}$$

Then, Eqs. (A1) through (A8) can be rewritten in a form suitable for the numerical calculations as

$$\begin{aligned} &A\eta^2 + B\eta + C = 0, \\ &\eta = [-B \pm (B^2 - 4AC)^{1/2}]/2A \\ &A = R_{12}^{(p)} R_{12}^{(s)} (\rho r_{01}^{(p)} - r_{01}^{(s)}) \\ &B = r_{01}^{(s)} r_{01}^{(p)} (\rho R_{12}^{(p)} - R_{12}^{(s)}) + \rho R_{12}^{(s)} - R_{12}^{(p)} \\ &C = \rho r_{01}^{(s)} - r_{01}^{(p)}\ . \end{aligned} \tag{A9}$$

From Eq. (A9), we find

$$d_1 \equiv d_{\mathrm{ad.layer}} = (\lambda/4\pi)[i\ln\eta/(n_1^{*2} - n_0^2 \sin^2\theta_0)^{1/2}], \quad \mathrm{Im}(i\ln\eta) = 0,\ n_1 \equiv n_{\mathrm{ad.layer}} \tag{A10}$$

The thickness of the adsorbed layer and the refractive index of the adsorbed layer may be found simultaneously from Eqs. (A10).

## Appendix B

The adsorbate density in the adsorbed layer decreases with increasing distance from interface [20–22]. Therefore, the adsorbed layer is not homogeneous and the refractive index $n_{\text{ad.layer}}$ and thickness $d_{\text{ad.layer}}$ of the adsorbed layer represent optical average values, i.e., $\bar{n}_{\text{ad.layer}}$ and $\bar{d}_{\text{ad.layer}}$, which the ellipsometric technique may find. The physical meaning of $\bar{n}_{\text{ad.layer}}$ and $\bar{d}_{\text{ad.layer}}$ for various adsorbate and polymer mixtures with various segment distribution has been discussed by McCrackin and Colson [23].

The molar refraction of the adsorbed layer $R^*_{\text{ad.layer}}$, consisting of a mixture of solvent and adsorbate, can be found by using the Lorentz-Lorenz equation [13]

$$R^*_{\text{ad.layer}} = \alpha_{\text{sol}} R^*_{\text{sol}} + \alpha_{\text{absorbate}} R^*_{\text{adsorbate}} \tag{B1}$$

$$R^*_{\text{i}} = V_{\text{i}} R_{\text{i}},\ R_{\text{i}} = (n_{\text{i}}^2 - 1)/(n_{\text{i}}^2 + 2)\,, \tag{B2}$$

where $\alpha_{\text{i}}$ and $V_{\text{i}}$ are the mole fraction and the volume of the solvent and adsorbate, respectively; $n_{\text{i}}$ is the refractive index of component $i$. The volume of the adsorbed layer is given by

$$V_{\text{ad.layer}} = \alpha_{\text{sol}} V_{\text{sol}} + \alpha_{\text{adsorbate}} \xi V_{\text{adsorbate}}\,, \tag{B3}$$

where $\xi$ is the ratio of the adsorbate volume in the adsorbed layer and in the bulk.

The parameter $\xi$ characterizes the change (or compression) of the adsorbate density in the adsorbed layer. The weight fraction $X_{\text{i}}$ of the substance $i$ is given by

$$X_{\text{i}} = c_{\text{i}}/\rho_{\text{i}}\,, \tag{B4}$$

where $c_{\text{i}}$ is the weight concentration of the substance $i$ in gram per volume ($g/\text{cm}^3$) and $\rho_{\text{i}}$ is a density of the substance $i$ ($g/\text{cm}^3$).

From Eqs. (B1) through (B4), we find

$$R_{\text{ad.layer}}\alpha_0 = X_{\text{sol}} R_{\text{sol}} + X_{\text{adsorbate}} R_{\text{adsorbate}}, \quad \alpha_0 = X_{\text{sol}} + \xi X_{\text{adsorbate}}\,, \tag{B5}$$

where $X_{\text{adsorbate}}$ is the weight fraction of the adsorbate in the adsorbed layer. If a density of adsorbate is the same in the adsorbed layer and in the bulk, then $\xi = 1$ and $\alpha_0 = 1$.

From Eqs. (B1) through (B5) it follows that the refractive index in the adsorbed layer $n_{\text{ad.layer}}$ depends on the polymer concentration in the adsorbed layer in the complex manner. In fact, from Eqs. (5) the derivative $\beta$ is equal to

$$\beta = dn_{\text{ad.layer}}/dX_{\text{adsorbate}} \approx (R_{\text{adsorbate}} - R_{\text{sol}})(n^2_{\text{ad.layer}} + 2)^2/(6\alpha_0 n_{\text{ad.layer}})\,. \tag{B6}$$

However, as first approximation for low adsorbate concentration, we may assume that $\beta$ is constant and the refractive index of the adsorbed layer $n_{\text{ad.layer}}$ depends on the adsorbate concentration in the linear form, i.e.,

$$n_{\text{ad.layer}} = n_{\text{sol}} + \beta \Delta c_{\text{adsorbate}}/\rho_{\text{adsorbate}},\ \Delta c_{\text{adsorbate}} = c_{\text{adsorbate}} - c_{0.\text{adsorbate}}\,, \tag{B7}$$

where $c_{0.\text{adsorbate}}$ is the adsorbate concentration in the bulk.

According to McCrackin and Colson [23], the average thickness of the adsorbed layer $\bar{d}_{\text{ad.layer}}$ is given as

$$\bar{d}_{\text{ad.layer}} = \int_0^\infty [n_{\text{ad.layer}}(X) - n_{\text{sol}}]dx / \times (\bar{n}_{\text{ad.layer}} - n_{\text{sol}})\,, \tag{B8}$$

where $n_{\text{ad.layer}}(X)$ is the refractive index in the adsorbed layer which is a function of the distance $x$ from the surface ($x = 0$). From Eq. (B8), we find

$$\int_0^\infty [n_{\text{ad.layer}}(X) - n_{\text{sol}}]dx = \bar{d}_{\text{ad.layer}}(\bar{n}_{\text{ad.layer}} - n_{\text{sol}}) \tag{B9}$$

The adsorbed amount per unit of surface, $\Gamma$, is given by

$$\Gamma = \int_0^\infty \Delta c_{\text{adsorbate}}(x)dx,\ \Delta c_{\text{adsorbate}} = c_{\text{ad.layer}} - c_{0.\text{adsorbate}}\,. \tag{B10}$$

If the dimension of $\Gamma$ is mole per unit of surface, then from Eqs. (B7) through (B10), we find

$$\Gamma = \bar{d}_{\text{ad.layer}}(\bar{n}_{\text{ad.layer}} - n_{\text{sol}})\rho_{\text{adsorbate}}/(\beta M_{\text{adsorbate}}) \approx \bar{d}_{\text{ad.layer}}\rho_{\text{adsorbate}} X_{\text{adsorbate}}/M_{\text{adsorbate}} \tag{B11}$$

$$X_{\text{absorbate}} \approx 6 n_{\text{ad.layer}}(\bar{n}_{\text{ad.layer}} - n_{\text{sol}}) / \times [(R_{\text{absorbate}} - R_{\text{sol}}) \times (n^2_{\text{ad.layer}} + 2)^2]\,, \tag{B12}$$

where $X_{\text{absorbate}}$ is the weight fraction of adsorbate in the adsorbed layer; $M_{\text{absorbate}}$ is the molecular weight of the adsorbate.

## References

1. Drago RS, Vogel GC and Needham TE (1987) J Am Chem Soc A93:6014
2. Berg JC (1993) in Wettability (Berg JC Editor) Marcel Dekker, New York 49:75

3. Pearson RG (1963) J Am Chem Soc 85:3533
4. Fowkes FM (1987) J Adhesion Sci Tech 1:1
5. Zisman WA (1964) in Contact Angle, Wettability and Adhesion. Advances in Chemistry (Fowkes FM Chairman, Gould RF Editor) Amer Chem Soc 43:1
6. Fowkes FM (1964) in Contact Angle, Wettability and Adhesion. Advances in Chemistry (Fowkes FM Chairman, Gould RF Editor) Amer Chem Soc 43:99
7. Wilkonson F (1972) J Colloid Interface Sci 40:14
8. Filippov LK and Filippova IV (1986) Russian Journal Physical Chemistry 60:1842
9. Hiemenz PC (1987) Principles of Colloid and Surface Chemistry Marcel Dekker, New York:94
10. Azzam RM and Bashasa NN (1977) Ellipsometry and Polarized light North-Holland, Amsterdam:75.
11. So S and Vedam K (1972) J Optical Society Am 62:16.
12. Reddy AK and Bockris OM (1964) Ellipsometry in the Measurement of Surfaces and thin films National Bureau of Standards Technical Note 256, National Bureau of Standards, Washington DC.
13. Born M and Wolf E (1965) Principles fo Optics Pergamon Press, New York
14. Fleer GJ and Lyklema J (1983) in Adsorption from solution and the Solid/Liquid Interface (Parfitt GD and Rochester CH Editors) Academic Press, London Ltd 2:153
15. Lipatov YuS and Serggeva LM (1974) Adsorption of Polymre John Wiley, New York 4:143
16. Langmuir I and Schaefer S (1937) J Am Chem Soc 59:2400
17. Ward AFG and Tordai L (1946) J Chem Phys 14:453
18. Hansen RS (1960) J Phys Chem 64:637
19. Filippov LK (1994) J Colloid Interface Sci 163:49
20. Vasicek A (1960) Optics of Thin Films North-Holland Press, Amsterdam
21. Passaglia RR and Kruger J (1964) Ellipsometry in the Measurement of Surfaces and thin films National Bureau of Standards Technical Note 256, National Bureau of Standards, Washington DC.
22. De Feijter JA, Benjamins J and Veer FA (1978) Biopolymers 17:1759.
23. McCrackin FL and Colson JP (1964) Ellipsometry in the Measurement of surfaces and thin films National Bureau of Standards Technical Note 256, National Bureau of Standards, Washington DC

Received November 8, 1993;
accepted November 1, 1994

Author's address:

Leonid Filippov, Sc.D.
510 Seneca St.
First Floor
Bethlehem, Pannsylvania, 18015, USA